ELSEVIER

Thermochimica Acta 364 (2000) 181–191

thermochimica acta

www.elsevier.com/locate/tca

Reversing melting and crystallization of indium as a function of temperature modulation☆

R. Androsch[a], B. Wunderlich[b,*]

[a]*Martin-Luther University, Halle-Wittenberg, Institute of Material Science, Geusaer Street, Merseburg 06217, Germany*
[b]*Department of Chemistry, The University of Tennessee Knoxville, Knoxville, TN 37996-1600, and Oak Ridge National Laboratory, Chemical and Analytical Sciences Division, Oak Ridge, TN 37831-6197, USA*

Received 25 March 2000; received in revised form 14 August 2000; accepted 20 August 2000

Abstract

The melting and crystallization of indium has been reinvestigated with the heater-controlled Mettler–Toledo differential scanning calorimeter DSC 820. The heat-flow rate during melting and crystallization is largely determined by instrumental characteristics and often does not permit the evaluation of kinetic parameters of the phase transition. We found that the observed reversing character of the melting depends strongly on the modulation parameters. For quasi-isothermal, temperature-modulated calorimetry with a symmetric sawtooth, the degree of reversibility decreases with increasing amplitude of temperature modulation. At a lower average temperature of modulation relative to the melting temperature, the partial melting process can be fully reversing, while at higher average temperatures, the melting becomes less reversing due to instrumental time restrictions for the completion of melting. With an appropriately modified, nonsymmetric sawtooth, however, the phase transition can be made fully reversing, even in the later stages of the melting process (as long as crystal nuclei remain). The influence of sample mass, sample position within the pan, and type of pan are analyzed, and the conditions for the study of the kinetics of crystallization of nucleated crystals close to the melting temperature, and by implication, also the melting kinetics, are suggested. Published by Elsevier Science B.V.

Keywords: Melting; Crystallization; Indium; DSC; TMDSC

1. Introduction

Standard differential scanning calorimetry (DSC) and the recently introduced extensions to the temperature-modulated DSC (TMDSC) are frequently used methods for the study of the kinetics and reversibility of first order transitions[1] [1]. According to the laws of equilibrium thermodynamics, the temperature of a one-component sample must remain constant until the crystallization or melting is completed, i.e. as long as two phases coexist (Gibb's phase rule) [1]. The measured heat-flow rate during melting and

☆The submitted manuscript has been authored by a contractor of the US Government under the contract no. DE-AC05-96OR22464. Accordingly, the US Government retains a non-exclusive, royalty-free license to publish, or reproduce the published form of this contribution, or allow others to do so, for US Government purposes.

* Corresponding author. Present address: Department of Chemistry, The University of Tennessee, Knoxville, TN 37996-1600, USA. Tel.: +1-865-974-0652; fax: +1-865-974-3419.
E-mail address: athas@utk.edu (B. Wunderlich).

[1] For an update and extension, see also, Thermal Analysis of Materials, a computer-assisted lecture course of 36 lectures on 2879 screens, downloadable from the internet including presentation software, web.utk.edu/~athas/courses/tham99.html, The University of Tennessee, Knoxville, 2000.

0040-6031/00/$ – see front matter Published by Elsevier Science B.V.
PII: S0040-6031(00)00644-4

crystallization, however, is governed by sample and instrument properties, i.e. the total latent heat, the thermal resistance within the sample, and the paths between sensor, heater, and sample, as well as the experimental parameters such as the heating rate and modulation amplitude [2,3]. Hence, the DSC data during a first-order transition represent never an infinitely sharp peak, as required by the phase rule, but vary for different types of calorimeters and experimental parameters. A shorter heat conduction path, i.e. a lower thermal resistance between heater and sample, reduces the time constant of the instrument and shortens the necessary time for the sample to complete the transition. Furthermore, a DSC can be controlled by sensors either close to the heater or close to the sample. In the latter case, the power of the heater is increased or decreased substantially during transitions, shortening the time the calorimeter is out of control during the transition.

The influence of the thermal resistances between the heater, sensor, and sample on the heat-flow rate during first-order transitions is well established for the standard DSC and TMDSC. Equations have been derived to extract correct heat capacities considering the behavior of the instrument [4–7]. In the present study, we attempt to explore the melting and crystallization behavior of indium by quasi-isothermal TMDSC, using a calorimeter with small thermal resistance between the heater and the sensor, but a large thermal resistance between heater and sample, as found in the Mettler–Toledo heat flux DSC 820. We try to show the influence of the modulation parameters on the reversing response to the crystallization and melting transition, in particular, as affected by the shape and the symmetry of the applied sawtooth modulation. Later, we plan to compare the results obtained with the heater-controlled heat-flux instrument with data obtained with a sample-temperature controlled power-compensation calorimeter. With these studies, we continue our broad effort to understand the complex nature of a TMDSC experiment during first-order transitions.

In the present research, we used indium, to be able to compare the results with earlier studies with the same calorimeter [8] and related ones with a sample-temperature controlled heat-flux DSC [9]. In the present paper, which deals with the attenuation of the modulation amplitude and the phase lag caused by sample thickness, we present proof which supports the recently performed surface temperature measurements using infrared thermography [10] and calculations [11,12] indicating a considerable smearing of the heat-flow data during the crystal-melt transition.

The TMDSC is a useful thermal-analysis tool to separate processes of different kinetics by exposing a sample simultaneously to different heating rates, q: (1) an underlying heating rate in the range between 0 and 5 K min^{-1} and (2) a periodically changing heating rate, corresponding to a modulation amplitude in the range between 0.1 and 5 K and a modulation period between 10 and several hundred seconds [13–15]. The resultant heat-flow rates usually are separated by a discrete Fourier transformation into total, reversing, and nonreversing components. The total component is the average of one period and is given by the 0th Fourier coefficient, and the reversing component of the heat-flow rate is defined as the amplitude of the 1st harmonic of the Fourier series, i.e. the reversing component filters the events which are able to be completely or partially modulated at the selected frequency. The term reversing is used instead of the term reversible to mark the frequent difference of the observed data from the truly thermodynamically reversible events. While a reversible process must be reversing, the reverse is often not true. The total and reversing components of the heat-flow rate are recalculated in terms of apparent heat capacities via division with the underlying heating rate and amplitude of the first harmonic of the modulated heating rate, respectively. In addition to the temperature- and heat-flow-rate calibration, as customary for a standard DSC, the calculation of the reversing heat capacity requires a frequency calibration [6,7]. In case of quasi-isothermal TMDSC, total as well as nonreversing apparent heat capacities cannot be calculated from an irreversible heat-flow because of the constant base temperature, T_0.

The thermodynamic reversibility of the crystal to melt transition is controlled by the chemical structure of the material studied and the crystal nucleation barriers. In case of flexible polymers, the transition is additionally irreversible due to the need of molecular nucleation, which is expressed by an additional supercooling of usually 10–20 K [1,16,17]. Consequently, in TMDSC, the heat-flow rate associated with

the latent heat of the crystal-melt transition is inherently irreversible, but may become partially reversing on appropriate nucleation. A small amount of truly reversible crystallization and melting in polymers has been observed by TMDSC and by small-angle X-ray scattering [18–21] (<1% crystallinity-change per kelvin), however, it is probably restricted to the existence of a specific morphology of the crystal surface. Liquid crystals, in contrast, exhibit often a thermodynamically reversible isotropization transition [18]. In case of metals like indium, the focus of the present study, crystallization is irreversible in the absence of nuclei, but with a much smaller super-cooling than for polymers, and may become reversible in the presence of nuclei and at sufficiently small rates of temperature change so that the crystallization and melting kinetics are not limiting [8,9].

In prior DSC and TMDSC experiments with a sample-temperature-controlled heat-flux calorimeter [9], it was shown that (1) the required supercooling after complete melting is 1–2 K, and (2) that the onset of crystallization and melting can be reversible as long as crystal nuclei remain. Similar measurements were performed using the same heater-controlled heat-flux calorimeter as in the present study [8]. The present data are in agreement with the formerly gathered results about the supercooling of completely melted indium and the reversibility of the phase transition as long as nuclei remain. In the present research, we extent these studies and present detailed information on the apparent time dependence of the phase transition. It will be shown that the apparent degree of reversibility of a phase transformation strongly depends on the modulation parameters which cause instrumental restrictions, and the true melting and crystallization rates.

2. Experimental

TMDSC experiments were performed using a Mettler–Toledo DSC 820 with the ceramic sensor FRS 5, controlled at the heater. The instrument was operated with the liquid nitrogen accessory. The furnace and the DSC cell were purged with dry nitrogen and air, respectively, both at a flow rate of 80 ml min^{-1}. The temperature was calibrated using indium and zinc, including the so-called tau-lag calibration which corrects lags due to the heating rate. The heat-flow rate was calibrated with the enthalpy of fusion of indium. The TMDSC was used in the quasi-isothermal sawtooth-modulation mode. Preferred modulation parameters were set at 0.05 K modulation amplitude and 0.25 K min^{-1} heating and cooling rates within the sawtooth, which result in a modulation period of 48 s. The temperature-step between successive average temperatures was 0.1 K, and before the modulation, the sample was kept isothermally for a period of 3 min at the initial, minimum-temperature (see Fig. 2a). This symmetry of the sawtooth was modified (a) by insertion of isotherms of different lengths at the end of the cooling segment (see Fig. 4b), (b) by variation of the maximum temperature of the heating segment, or (c) by insertion of isotherms of different length at the end of the heating segment (see Fig. 5). We have used samples of 0.59, 1.04, 2.77, and 6.55 mg to explore the influence of the amount of enthalpy of fusion. In every case the sample was flattened to optimize the heat conduction. In all measurements closed, 40 μl aluminium pans of about 48 mg with a center pin were used. Supplemental experiments to check the reproducibility of the data were performed with the smaller pan of aluminium and with a volume of 20 μl, covered and uncovered (≈28 mg). The sample was located at different positions within the pan. The data were not baseline-corrected since a conversion into heat capacities is not necessary for the discussion of the reversibility of the transition. Any instrumental drift during the experiments is corrected by subtraction of a virtual baseline. The indium used in this study has a purity of 99.999% and a melting temperature of 429.75 ± 0.1 K. Note, that in the following discussion we use the widely applied term *sample temperature* for the temperature which is measured by the sensor in close proximity to the sample, and which is not necessarily the true temperature within the sample, as was shown even for samples not undergoing transitions by measuring the sample temperature externally [10]. We follow in this aspect, the nomenclature of all major instrument providers (although it is not precise). The legends within the figures contain all necessary experimental parameters in abbreviated form, i.e. amp: amplitude in K, rate: modulated heating-rate in K min^{-1}, per: modulation-period in s, and (#×): the number of repetitions.

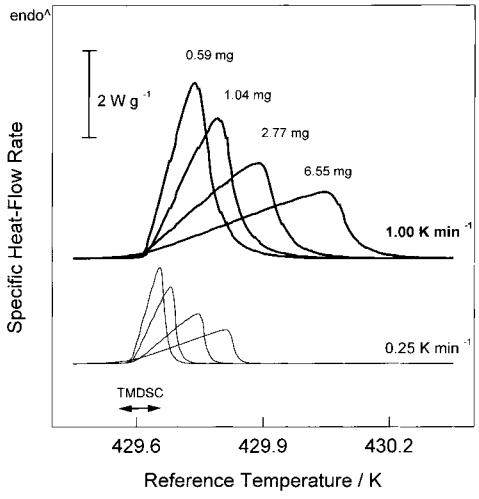

Fig. 1. Melting of indium as a function of mass at 1.00 and 0.25 K min^{-1}. Note that the specific heat-flow rate is given in W g^{-1}. For the heat-flow rate given in W, the leading edges of all curves would all have close to the same slope.

3. Results and initial discussion

Fig. 1 presents an overview of the standard DSC traces of the melting behavior of indium samples of different mass using heating rates, q, of 1.00 and 0.25 K min^{-1} (upper and lower curves, respectively). The measurements demonstrate the mass and heating-rate dependence of the melting process, as described and analyzed in standard text books [1–3]. For a given heating rate, the rate of maximum heat-flow caused by the constant melting temperature of the sample is fixed, as was also demonstrated in [8]. As a result, the slope of the specific heat-flow rate (per gram of the sample) decreases with sample mass due to the increased total latent heat absorbed by the sample as a whole. The result is a longer time for complete melting of heavier samples. Increasing the heating rate increases the temperature range for melting, while the slope of the melting peak remains the same, as expected (see Section 4.4.2 of [1]). The abscissa in Fig. 1 represents the program temperature which is also the reference temperature and keeps increasing linearly, unaffected by the phase transition. The sample temperature, in contrast, should remain constant as long as the transition is not completed, i.e. crystal and melt coexist. The double arrow at the bottom of the figure marks the applied modulation amplitude in the following TMDSC experiments.

The same experiments carried out with a heat-flux DSC which is governed by the sample temperature, in contrast, would increase the heat-flow rate as soon as melting begins, in an effort to keep the heating rate of the sample constant. This instrument-caused change results in a higher heating rate in the reference calorimeter. Naturally, the thermodynamics of the transition does not permit a true achievement of this goal, and the temperature gradient between the sample, melting at T_m, and the sample-temperature sensor is in this case limiting the heat-flow rate as long as the heater has not reached its maximum power.

Fig. 2a and b show the melting and crystallization process of indium during quasi-isothermal modulation at step-wise increasing temperatures. Fig. 2b magnifies the final melting range which is indicated by the rectangle in Fig. 2a. The lower curves are the modulated heat-flow rates (use the left ordinate) and the upper curves (use the right ordinate) represent the reference temperatures (programmed temperatures, represented by the thin line) and the sample temperatures (given by the thick line). The quasi-isothermal modulation at each average temperature was performed for 15 cycles and is followed by a 3-min isotherm at the maximum temperature, before initiating the next modulation cycles at a 0.1 K higher average temperature. The isotherms prior to the modulation, shown in the plot, are at 429.26, 429.36, 429.46, and 429.56 K. The modulation is symmetric, i.e. the heating and cooling rates both are 0.25 K min^{-1}. The first 15 cycles at about 429.31 K reveal a small heat-flow-rate amplitude which results from the heat capacity and the asymmetry of the instrument (baseline).

An increase of the average temperature by 0.1 K–429.41 K, shows a slightly increased amplitude of the specific heat-flow rate. The increase of the amplitude of the heat-flow rate is due to a small amount of reversing melting and crystallization with a latent heat of less than 0.1 J g^{-1}.

The next modulation between 429.46 and 429.56 K results in a considerably larger amplitude of reversing, specific heat-flow rates with a latent heat of about 0.5 J g^{-1}. After the last modulation segment, the sample continues to melt with an enthalpy of fusion of about 0.5 J g^{-1} during the first minute of the

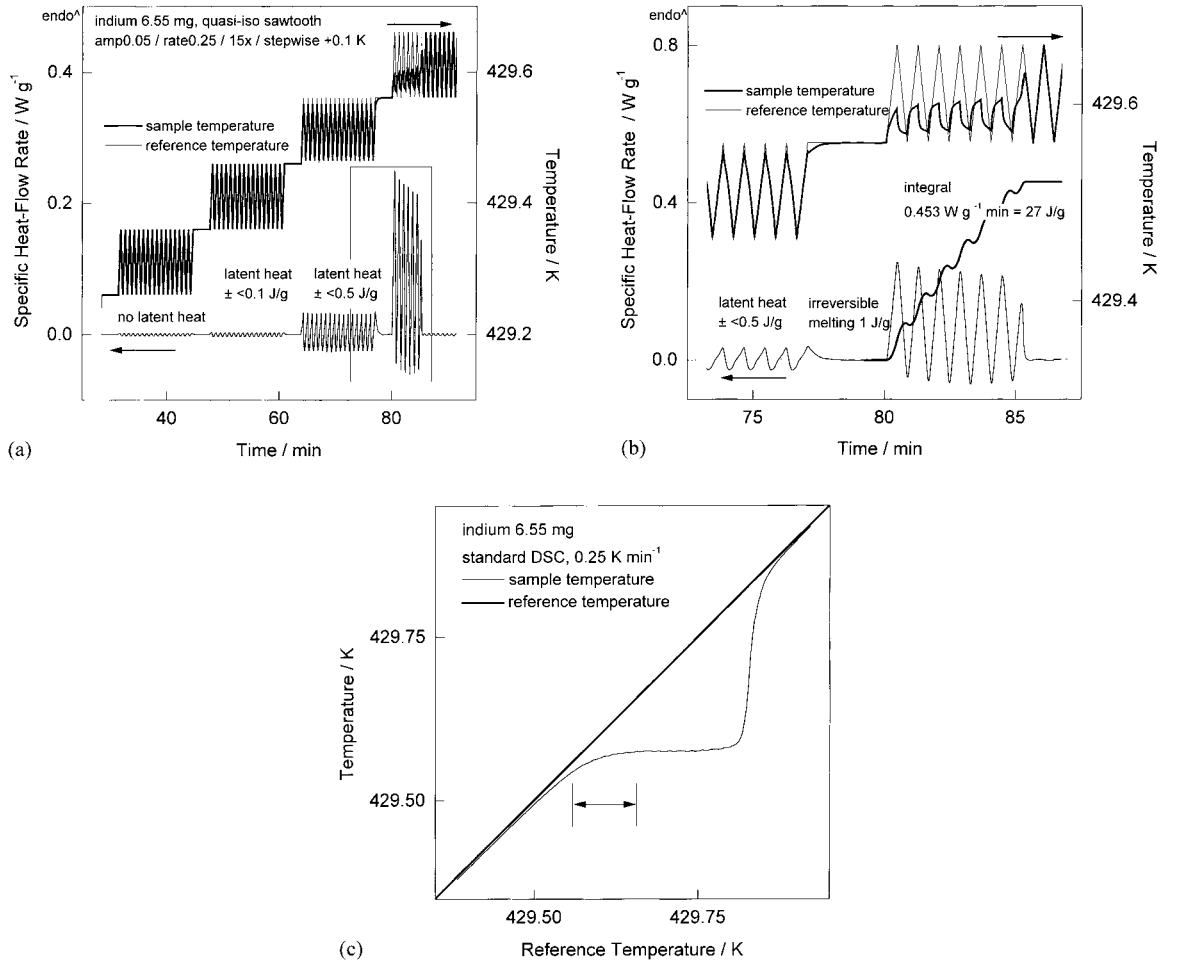

Fig. 2. (a) Plot of the modulated specific heat-flow rate (left ordinate, lower curve) and modulated reference and sample temperatures (right ordinate, upper curves), both vs. time during melting of indium of mass 6.55 mg. (b) Expansion of part of the final melting range of indium seen in Fig. 2a. (c) Sample temperature vs. reference temperature. Standard DSC curve during the melting of indium of mass 6.55 mg at 0.25 K min^{-1}. The double arrow marks the quasi-isothermal modulation range for TMDSC at 429.61 K (see Fig. 2a and b).

isotherm (see Fig. 2b). This increases the total enthalpy of fusion absorbed up to 429.56 K to about 1.0 J g^{-1}. Half of this melting was not occurring during modulation because of the time limitation during the modulation.

The last modulation in Fig. 2b is between 429.56 and 429. 66 K. It illustrates the final melting event. The amplitude of the specific heat-flow rate is initially considerably larger than at 429.51 K, and decreases continually with time. Ultimately, it abruptly recovers the value caused by heat-capacity and asymmetry before the 15-cycle modulation is finished.

Fig. 2b contains the integral heat-flow as a function of time, which illustrates the course of melting and the limited reversing during the modulation about the average temperature of 429.61 K. As expected, the measured sample temperature does not follow the programmed modulation as long as melting and crystallization continues. Note that almost the entire modulation cycle has an endothermic heat-flow response and crystallization occurs only at the very end of each cooling segment. The process is, thus, almost fully non-reversing, making the customary data-evaluation process to extract

reversing events by Fourier transformation meaningless [8].

Furthermore, we need to point to the relatively small, but distinct modulation recorded by the sample temperature sensor. Albeit, the sample temperature, should remain constant during entire transition, some of the modulation of the heater temperature clearly is forwarded to the sample. The apparent modulation of the sample temperature must be caused by setting up of a temperature gradient within the melted layer that separates the remaining crystals of indium from the sample pan [10]. The double arrow in Fig. 2c marks the modulation range of the recorded sample temperature generated by standard DSC at the same heating rate and sample mass as used for the TMDSC. On TMDSC, the sample sensor barely reaches the (almost) constant level within the modulation of 0.05 K and modulates this temperature region due to the repeated interruption and re-start of the melting process by superheating and supercooling of the already melted outer layer of indium. The thickness of the liquid indium layer may be estimated from the slight deviation from a horizontal of the thin line of the sample temperature in Fig. 2c. The gradual approach of the sample sensor temperature on the standard DSC from steady state of heating of the crystal (up to about 429.45 K) to the steady state of melting with slowly increasing amounts of liquid indium (at about 429.55 K) can be caused to some degree by impurity of the sample, as well as by poorly grown crystals, but in this case of pure indium, most must be due the exponential approach to the new steady state, governed by the time constant of the calorimeter. The slowly changing steady state of melting was seen before [8], but only now are the chosen conditions precise enough to suggest that a quantitative analysis in terms of the layer thickness of the liquid indium separating the crystal might be possible.

Fig. 3 summarizes the influence of the sample mass on the final melting step when expressed as specific heat-flow rate. The insert shows the specific enthalpy of transition as function of time. As expected from the general functional relations governing the heat-flow into the sample, $\Delta H_f \propto q(\Delta t)^2$, where Δt is the time from beginning to end of melting, an increasing sample mass broadens the transition [1]. As discussed on the basis of Fig. 2a and b, the melting process is almost completely nonreversing and the total heat-

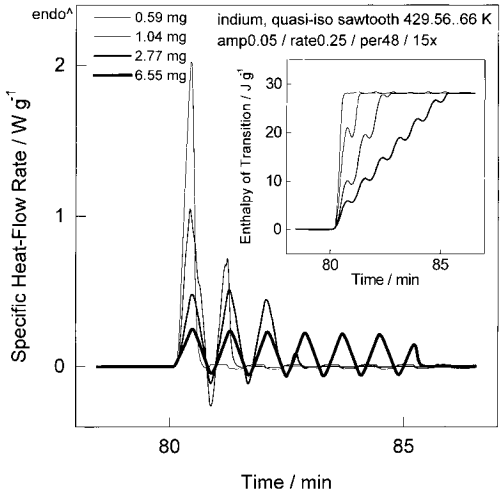

Fig. 3. Modulated specific heat-flow rate vs. time in the final melting range of indium of different masses. The insert shows the change in enthalpy of transition as function of time.

flow rate (the specific heat-flow rate multiplied by mass) has practically constant slopes for all masses.

Next, a similar symmetric modulation experiment as in Fig. 2 is modified by the insertion of isotherms in the last melting sequence. Fig. 4a shows the result with inserted isotherms of lengths from 0 to 5 min at the end of each cooling segment. Fig. 4b, again, is the enlargement covering the end and beginning of the last two modulation sequences, respectively. The top of the five curves is similar to the one of Fig. 2a. If an isotherm is inserted between the modulation cycles, the length of the overall melting process extends over many more cycles. In case the isotherm is shorter than 3 min, an incomplete crystallization component is evident in each modulation cycle, and by accumulation of the larger enthalpies of fusion, the melting process is completed before the end of the 15 modulations. In case, the isotherm is 3 min or longer, as in the lower two curves in Fig. 4, the melting process is fully reversed by the slow subsequent crystallization process. A small amount of the crystallization occurs at the end of the cooling segment, but most of it is seen during the isotherms. In Fig. 4c, the progress of the melting process is shown by an integral analysis of the enthalpy of transition as suggested in [8]. The rate of melting at 429.56 K in Fig. 4c, which is controlled by the true melting rate and instrumental restrictions (thermal resistance of the instrument and the sample),

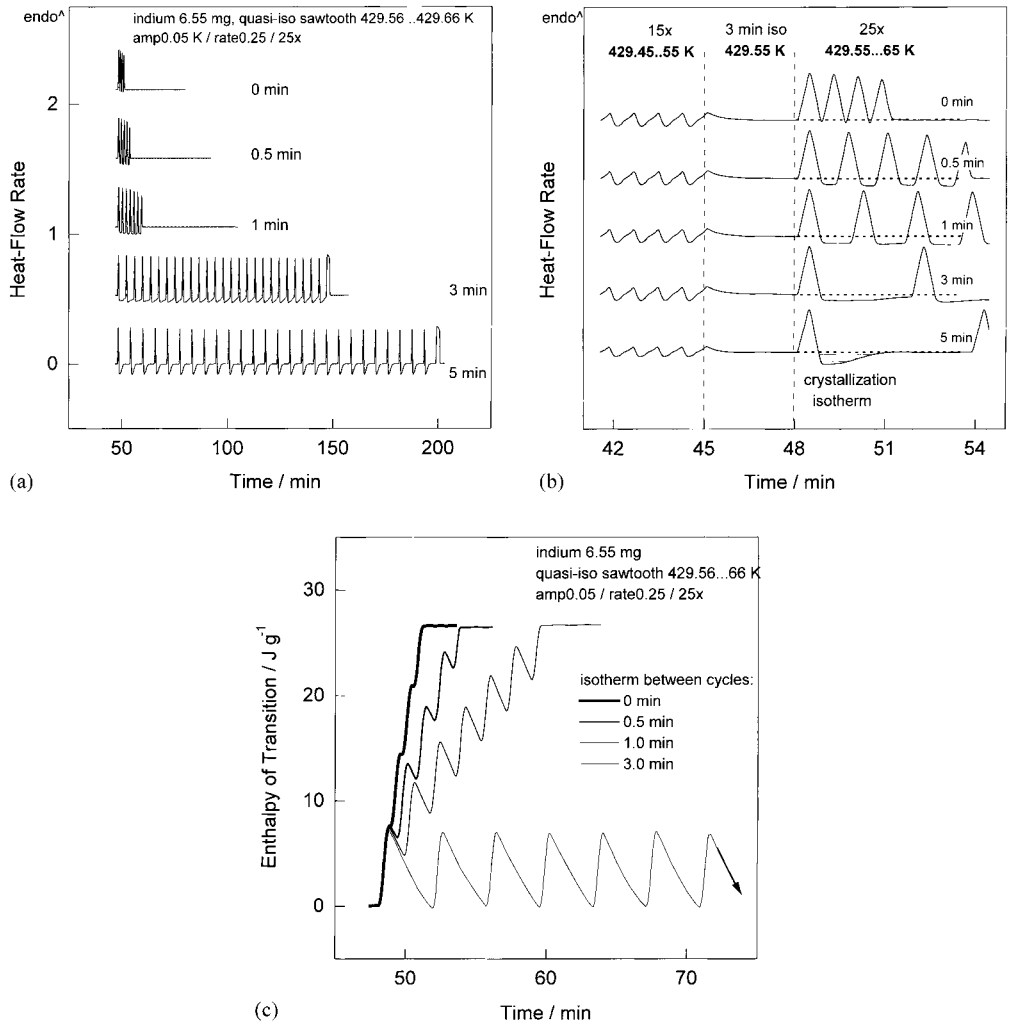

Fig. 4. (a) Plot of the modulated heat-flow rate vs. time obtained during melting of indium of mass 6.55 mg. The temperature program, which was used in the experiments of Fig. 2a and b was modified by insertion of isothermal segments during quasi-isothermal modulation between 429.55 and 429.65 K at the end of each cooling branch. The length of the isotherm changes from 0 min (upper curve) to 5 min (lowest curve). (b) Plot of the modulated heat-flow rate vs. time obtained during melting of indium. Enlarged part of Fig. 4a. (c) Enthalpy of transition as function of time during modulation between 429.56 and 429.66 K, calculated on basis of data as shown in Fig. 4a and b.

is constant for the four cases (0–3 min isotherms). The crystallization rates are similarly equal. The positive and negative slopes, however, are different, causing also a non-reversing character of the experiment if time for completion of the crystallization is not sufficient. If the isotherm is long enough, crystallization can be completed, i.e. the total enthalpy of transition becomes zero at the end of each modulation-plus-isotherm cycle.

With Fig. 5, we continue the discussion of the experiments by identifying the apparent melting and crystallization rates of indium. In the new experiments, a variable isotherm of 0–2 min was inserted at the *upper* temperature of the sawtooth at 429.66 K. This isotherm is then followed by completion of the sawtooth cycle by the decrease in temperature back to 429.56 K, and completion of the experiment with an unlimited isotherm at 429.56 K. In Fig. 5a, it is shown

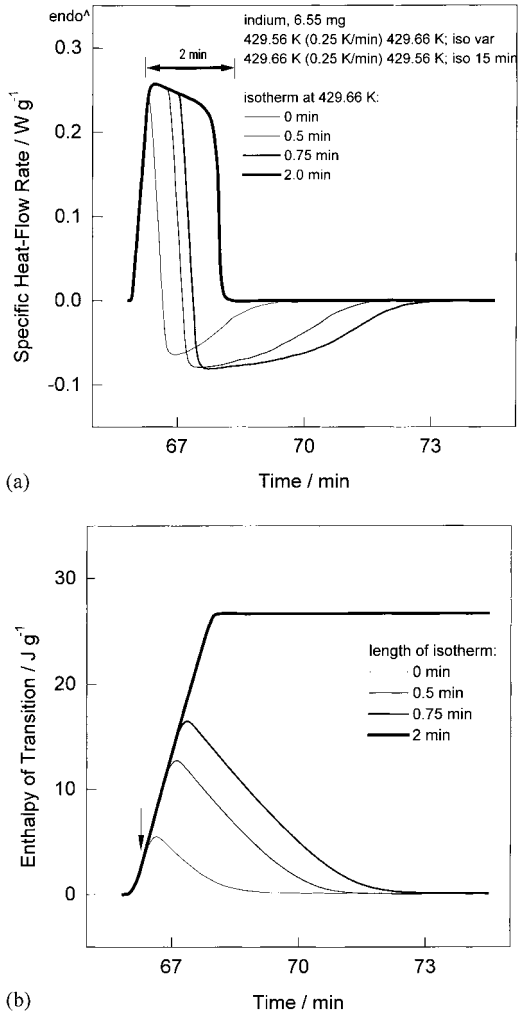

Fig. 5. (a) Plot of the modulated specific heat-flow rate as a function of time obtained during melting of indium of mass 6.55 mg. The temperature program, which was used in the experiments of Fig. 2a and b was modified by insertion of an isothermal segment of different lengths at the end of the first heating cycle at 429.66 K (0, 0.5, 0.75, and 2 min). (b) Enthalpy of transition as a function of time, integration of the data of Fig. 5a.

that the melting process extends over a period of almost 2 min if the reference temperature stays well above the almost constant sample temperature between 429.58 and 429.60 K (see sample temperature in Fig. 2b). As long as the melting process is not completed, as for the inserted upper isotherms of lengths 0, 0.5, and 0.75 min, cooling below the melting temperature permits renewed crystallization and, if the time for crystallization is sufficient, the process reverses fully. If the entire sample was melted, the subsequent cooling branch and isotherm cannot reverse the melting process due to the absence of nuclei. Fig. 5b is the integral of the data of Fig. 5a as a function of time. The increase of the enthalpy of transition is contiguous and independent of the temperature program, i.e. melting during the heating segment and the inserted isotherm is virtually indistinguishable. The temperature of 429.66 K is reached at the position of the arrow, and the increase of enthalpy of transition continues without break and discontinuity during the upper isotherm. As already mentioned in the discussion of Figs. 2b and 4c, the apparent melting and crystallization rates, as given by the positive and negative slope of the heat-flow curves, are different.

In a further experiment, which is not shown in the figures, we extended the heating branch which was beginning at 429.5 to 429.62, 429.68 and 429.72 K in the final melting range and followed the heating immediately by the cooling part of the sawtooth down to 429.56 K and an isotherm to allow for completion of the crystallization. The melting process is also similar to Fig. 5, i.e. once the true melting temperature is exceeded, melting is independent of the further temperature program.

Since the reversing of the melting and crystallization is dependent on the modulation parameters and the thermal resistance of instrument and sample, we tried to further explore the influence of instrumental parameters on the melting and crystallization behavior. As can be seen from Figs. 2–5, as soon as the true melting temperature is exceeded, the sample melts with a fixed, apparent rate which is almost independent of all further experimental parameters. The available total heat flux increases with decreasing thermal resistance of the instrument and sample, but, as can be seen from Figs. 1 and 3, is almost independent of variation of sample mass. The thermal resistance of the instrument may be altered by the choice of the pan type, by covering the pan, and by changing the position of the pan. In Fig. 6, the results are summarized that were obtained by changing these parameters. It clearly shows that (1) in case of the used heat-flux calorimeter with circularly arranged 56 thermocouples, the position of the sample (at the center or on the margin) seems unimportant, (2) the sample starts to

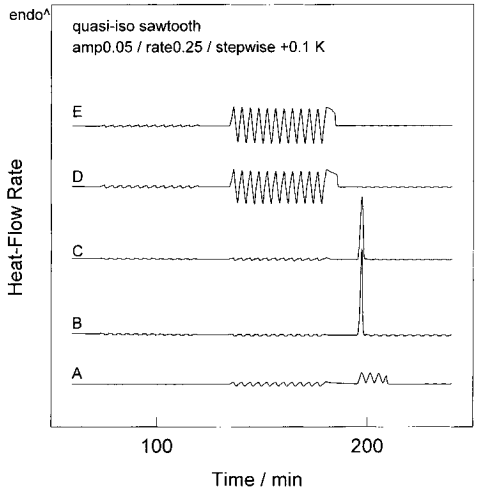

Fig. 6. Plot of the modulated heat-flow rate as a function of time: (A) heavy pan (48 mg), mass 6.55 mg, covered, sample centered; (B) heavy pan (48 mg), mass 0.56 mg, covered sample centered; (C) heavy pan (48 mg), mass $2 \times 0.5 = 1.0$ mg, covered, samples at margin of heat-flow sensor; (D) light pan (27 mg), mass 1.684 mg, covered; (E) light pan (27 mg), mass 1.684 mg, uncovered.

melt at a slightly lower temperature (0.05–0.1 K) if the light pan of 28 mg is used, and that (3) the highly conductive cover does not influence the melting behavior.

From these data, we conclude that the width of the melting process, (somewhat more than 0.1 K) probably is not determined by temperature gradients within the sample, but rather by the thermal resistance of the instrument. The smaller aluminium pan obviously contributes to a reduction of thermal resistance of the instrument, which results in a slightly decreased final melting temperature, and supports the recently quantified instrumental-time constant which is about 2 s rad^{-1} less than that of the heavy aluminium pan [22].

4. Final discussion and conclusions

The primary scope of the presented study was the investigation of the relation between the symmetry of the temperature-modulation on the total and reversing parts of the heat-flow rate during the crystallization and melting of indium. The experiments, discussed on the basis of Figs. 2–5, have shown that the reversing nature of the crystal-melt transition of indium is strongly determined by the modulation parameters. The modulation parameters must affect any first-order transition due to the inherent thermodynamic characteristic of the transition, namely the constancy of the sample temperature during the transition. This, in particular, is true if the transition occurs over several modulation cycles, as is often suggested to be a condition for the measurement of a meaningful reversing and nonreversing component of the total heat-flow rate in experiments with an underlying heating rate. As soon as the temperature of the sample reaches the melting point, the sample temperature is maintained (see Fig. 2, neglecting the minor modulation of sample temperature with an amplitude of about 0.01 K). The reference or program temperature is found, furthermore, not to affect the melting kinetics, as long it is above the melting temperature. Melting only gets reversed if the temperature falls below the melting point and if there are remaining nuclei. Even if the heating rate is negative, melting will continue without change until the melting point is reached.

Assuming that both melting and crystallization rates are controlled by the total thermal resistance of the system and are equal and independent of temperature, the reversing of the transition depends mainly on the amplitude of the quasi-isothermal modulation and the position of the melting temperature between the minimum and maximum of the modulation. Fig. 7 summarizes the two cases of reaching partial (lower curve) and full reversing (upper curve). If the transition occurs above the average of the modulated temperature, crystallization can reverse the melting as long as the melting is not complete and nuclei remain. If the transition occurs below the average temperature, almost the entire modulation cycle permits melting, and crystallization is largely suppressed. Needless to say that similar considerations hold for TMDSC experiments with an underlying heating rate. If the symmetry of the modulation is altered, as shown in Figs. 3–5, the ratio of melting to crystallization is distorted.

The Heat-flow-rate data on modulation about $T_0 = 429.51$ K on the left side of Fig. 2b, and also the results in [8], show that apparent crystallization is faster than the melting, as proven by the larger slope of the cooling cycle. The isothermal crystallization with

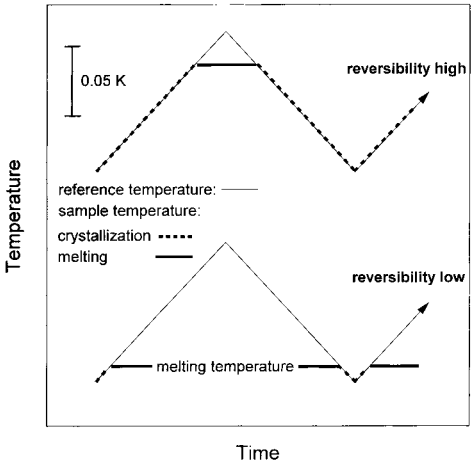

Fig. 7. Schematic of the reference (thin line) and sample temperature (bold line) as function of time during quasi-isothermal modulation with a symmetric sawtooth covering the true melting temperature.

a small supercooling, in addition, can be much slower than the instrument-limited heat flux. These effects are explained by the different limits of heat-flow rates on heating and cooling during the transition. On heating, the latent heat must be conducted into the sample through its surface at almost constant temperature. On cooling, in contrast, the latent heat is generated throughout the melt, at a rate limited only when reaching the melting temperature, i.e. when the heat generated in the sample reverses the programmed temperature decrease. It was shown, however, in [8] that only under special conditions, and even then only for short periods of time, can such crystallization generate a sufficient temperature increase to keep the sample at the melting temperature. The increasing supercooling, thus, speeds up the crystallization, while the melting is governed by a fixed local temperature gradient.

Figs. 4 and 5, in contrast, present isothermal crystallization experiments and one should be able to extract experimental rates of crystallization at very small amounts of supercooling within the limits of setting the isothermal temperatures as shown in Fig. 4b. Once, having established the value of the asymmetric sawtooth modulation, consisting of constant rates of temperature change and isotherms, it should be possible to limit the sample size for melting, so that the limiting heat-flow rate into the total sample is not exceeded. Under such conditions, it should also be possible to measure true melting rates. The study of superheating and of melting rates is of considerable interest in the polymer field where strained samples may show large temporary changes in superheating [17]. A series of earlier experiments in this area has established the value of superheating analyses for the characterization of polymers [23,24]. In the future, we hope to attempt to extract the kinetics of crystallization and melting based on the present analysis for polymers and non-polymeric samples. Although in the present investigation we have used a heater-controlled heat-flux DSC, the derived conclusions also should hold for other type of calorimeters, such as the sample-temperature-controlled heat-flux and power-compensated instruments.

Acknowledgements

This work was supported to a small part by the Division of Materials Research, National Science Foundation, Polymers Program, Grant No. DMR-9703692 and the Division of Materials Sciences, Office of Basic Energy Sciences, US Department of Energy at Oak Ridge National Laboratory, managed by Lockheed Martin Energy Research Corporation for the US Department of Energy, under contract number DE-AC05-96OR22464.

References

[1] B. Wunderlich, Thermal Analysis, Academic Press, New York, 1990.
[2] W.F. Hemminger, H.K. Cammenga, Methoden der Thermischen Analyse, Springer, Berlin, 1989.
[3] W.F. Hemminger, G. Höhne, Calorimetry, VCH, Weinheim, 1984.
[4] J.E.K. Schawe, W. Winter, Thermochim. Acta 298 (1997) 9.
[5] B. Wunderlich, Y. Jin, A. Boller, Thermochim. Acta 238 (1994) 277.
[6] R. Androsch, I. Moon, S. Kreitmeier, B. Wunderlich, Thermochim. Acta 357/358 (2000) 267.
[7] R. Androsch, B. Wunderlich, Thermochim. Acta 333 (1999) 27.
[8] A. Boller, M. Ribeiro, B. Wunderlich, J. Therm. Anal. 54 (1998) 545.
[9] K. Ishikiriyama, A. Boller, B. Wunderlich, J. Therm. Anal. 50 (1997) 547.
[10] R. Androsch, M. Pyda, H. Wang, B. Wunderlich, J. Therm. Anal. Calorim. 61 (2000) in print.
[11] F.U. Buehler, C.J. Martin, J.C. Seferis, in: K.R. Williams

(Ed.), Proceedings of the 26th NATAS Conference, Vol. 26, Cleveland, OH, 13–15 September 1998, p. 44.
[12] F.U. Buehler, J.C. Seferis, J. Therm. Anal. 54 (1998) 1.
[13] M. Reading, B.K. Hahn, B.S. Crowe, Method and Apparatus for Modulated Differential Analysis, US Patent No. 5,224,775 (1993).
[14] P.S. Gill, S.R. Sauerbrunn, M. Reading, J. Therm. Anal. 40 (1993) 931.
[15] M. Reading, D. Elliot, V.L. Hill, J. Therm. Anal. 40 (1993) 949.
[16] B. Wunderlich, Macromolecular Physics, Vol. 2, Crystal Nucleation, Growth, Annealing, Academic Press, New York, 1976.
[17] B. Wunderlich, Macromolecular Physics, Vol. 3, Crystal Melting, Academic Press, New York, 1980.
[18] B. Wunderlich, A. Boller, I. Okazaki, K. Ishikiriyama, W. Chen, M. Pyda, J. Pak, I. Moon, R. Androsch, Thermochim. Acta 330 (1999) 21.
[19] Y. Tanabe, G.R. Strobl, E.W. Fischer, Polymer 27 (1986) 1147.
[20] G.R. Strobl, M.J. Schneider, G. Voigt-Martin, J. Polym. Sci., Polym. Phys. 18 (1980) 1361.
[21] J.M. Schultz, E.W. Fischer, O. Schaumburg, H.G. Zachmann, J. Polym. Sci., Polym. Phys. 18 (1980) 239.
[22] R. Androsch, J. Therm. Anal. Calorim. 61 (2000) 75.
[23] E. Hellmuth, B. Wunderlich, J. Appl. Phys. 36 (1965) 3039.
[24] M. Jaffe, B. Wunderlich, in: E.F. Schwenker, P.D. Garn (Eds.), Thermal Analysis, Vol. 1 (Proceedings of the 2nd ICTA), Academic Press, New York, 1969, p. 387.